Empirical correlation for porosity deduction from X-ray computed tomography (CT)

Kazem Saadat [1], **Hossain Rahimpour-Bonab** [2] , **Mohammad Reza Esfahani** [1], **Jafar Vali** [1]
[1] *Exploration and Production Research Center, RIPI*
[2] *Department of Geology, University College of Sciences, University of Tehran, Tehran, Iran*
*Corresponding author, e-mail: saadatk@ripi.ir

Abstract
For obtaining reservoir petrophysical properties, for example porosity, non-destructive methods such as X-ray computed tomography, CT, seems to be precise and accurate. Porosity is deducted from the CT image with a single scan via different techniques, such as pore space detection by image segmentation techniques then correlation with porosity. More than one hundred samples with carbonate lithology have been scanned and analyzed in this study which leads to empirical correlation used for porosity calculation from CT data. The samples mainly grouped as dolostone, limestone and carbonate with respect to their mineral contents, having porosity ranges between 4.56 to 30.5 % and permeability from 0.25 to 3350.8 md. The results showed that the effect of atomic number is higher than the density on CT image. It is because density and atomic number in carbonate mineral (calcite and dolomite) show diverse relations. Thus, the assumption of known lithology would be a large source of error. A good linear relationship exists between the porosity and CT no. according to the developed correlations.

Key words: *Computed tomography (CT), Porosity, Dolestone, Limestone, Carbonate*

Introduction

The porosity is defined as the ratio of pore space volume to the total rock volume. There are several conventional methods for rock porosity determination. One of them is using the X-ray CT imaging. Image analysis and correlation technique are two methods to calculate porosity from a single CT scan. Computerized axial tomography (CT) or computer-assisted tomography (CAT) scanning is a nondestructive X-ray technology that produces an image of internal structure in a cross-sectional slice through an object by the reconstruction of a matrix of X-ray attenuation coefficients. The application of X-ray computed tomography (CT) imaging for porous media has been used for many years to study and understand the rock properties (Anderson et al., 19884; Peters and Afzal, 1992; John *et al.*, 1993; Ueta *et al.*, 2000). Porosity as one of these properties can be determined from X-ray CT measurements using either single-scan or multiple scan techniques. Withjack (1988) and Akin *et al.*, (2000) determined porosity by a dual scan at the same location obtained with different fluids saturating of porous medium. Akin *et al.*, (1996). proposed a method employing a dual scan at two energy levels. Another method that use a dual scan with a single energy level is described and discussed by Akin & Kovscek (2003). In the dual -scan technique, CT scans are carried out at the same physical location in a core sample at different known fluid saturations. The porosity at each location can be determined directly by performing a pixel by pixel subtraction of the two images and dividing by a calibration constant. If the two conditions are dry and evacuated (Sf = 0), and fluid saturated is one (Sf = 1) then equation 1, determined for the two saturation conditions, can be used to determine the porosity (Moss *et al.*, 1990).

$$\Phi = \frac{(CT_{wm} - CT_{am})}{(CT_{water} - CT_{air})} \qquad (1)$$

Where CT_{wm} is the CT number of water saturated sample and CT_{am} is the CT number of air saturated sample, CT_{water} the CT number of

water and CT_{air} the CT number of air. This technique removes any contribution caused by rock composition, negating the need for mineralogy information. In addition, the image subtraction technique greatly reduces the effect of beam hardening artifact (the noises and non coincidence of object boundaries with pixel boundaries) on the final results. Two drawbacks are the need to clean and dry the sample and the additional time needed for the experiment. The only limitation that the CT measurement places on the saturating fluid is that it must have a CT number much larger than the CT number of vacuum, which is essentially the CT number of air at one atmosphere (-1000 HU). Common oil field liquids, such as crude or refined oils or brines, can be used.

Single scan techniques is another method to obtain porosity, usually in homogeneous samples such as Berea sandstone (Wellington & Vinegar, 1987; Withjack, 1988). Correlations between CT number and porosity were mentioned by Hunt *et al.*, (1988). Two major benefits of single scan estimate of porosity are that they can be made using cores in native state and thus are less time consuming than the dual - scan measurements. However, accurate measurements require independent knowledge of small scale variations in core mineralogy and fluid saturations. Porosity estimates made without this knowledge, require several simplifying assumptions such as: single mineralogy; 2-only gas or liquid saturation. Consequently, a large source of error lies in the assumption of known lithology if the sample composed of various minerals, i.e. heterogeneous samples.

Method and Experimental Details
The porosity can be calculated from single CT scan data using either image analysis or correlation technique.

Image analysis
Porosity measurements by Image analysis with single scan of a rock is carried out by detecting the pore space through image segmentation techniques. Segmentation is the first treatment applied to CT images before analyzing the physical characterization. It consists of the pores spaces extraction in a given scale corresponding to the CT image resolution. This step is crucial because of the nature of the CT image and the sensibility of image segmentation techniques (Ashbridge *et al.*, 2003) . It can reduce or increase the pores space and blur or make the connection between them visible. The properties of the feature resulting from the segmented image can vary greatly with small changes in the segmentation parameters. Consequently, there is an uncertainty in the porosity measurement and its derived properties (Ashbridge *et al.*, 2003; Sheppard *et al.*, 2004).

Correlation technique
Correlation technique from CT image with a single scan is another way to calculate the porosity. In this method, the porosity from helium injection and average CT number of the core are correlated. An imaged slice can be divided into a matrix of volume elements (n×n voxels). The attenuation of Io X-ray photons passing through any single voxel having a linear attenuation coefficient μ reduces the number of transmitted photons to I according to Beer's law (Radaelli *et al.*, 2004):

$$I = I_o exp(-\mu x)$$
(2)

Where x is the dimension of voxel in the direction of the X-rays. Material parameters that determine the linear attenuation coefficient of a voxel (μ) include its density ρ and mass attenuation coefficient (μ_m):

$$\mu = \mu_m \rho$$
(3)

On the other hand, the linear attenuation coefficient is also a function of atomic number of the scanned object related to the mass attenuation coefficient. So that the linear attenuation coefficient μ can be expressed as:

$$\mu(E) = \rho Z^{3.8}\alpha(E) + \rho\beta(E) \qquad (4)$$

Where ρ and Z are the density and the atomic number of the scanned object respectively, and E is the X-ray energy. In addition, $\alpha(E)$ and $\beta(E)$ are also functions of the X-ray energy. Calcite and dolomite have effective atomic numbers 15.71 and 13.74, respectively, and their densities are 2.71 and 2.85 g/cm3, respectively (Coenen & Maas, 1994).

The atomic number of a multi-component sample is obtained from:

$$Z_e = \left(\sum f_i Z_i^{3.8} \right)^{1/3.8} \qquad (5)$$

Where, Z_e is the effective atomic number, Z_i is the atomic number of its elements and f_i is the corresponding fraction of electrons (Wellington & Vinegar, 1987).

If the image thickness and photon energy are kept constant, then the CT number of each slice is only affected by density and atomic number of the sample. It means that the porosity is the only parameter affecting CT number in a homogenous rock due to the differences between the density of pores and rock matrix (Demir Murat *et al.*, 2001):

$$CT_{avg} = CT_{matrix} * (1 - \Phi) + CT_{air} * \Phi$$

(6)

Experiments

Over one hundred samples with carbonate lithology including calcite, dolomite and anhydrite were taken under CT scan. They were grouped as dolestone, limestone and carbonate (mixed calcite, dolomite and anhydritic dolestone). The samples have porosity ranges from 4.56 to 30.5 % and permeability from 0.25 to 3350.8 mD. CT scan images of these samples include cross-sections in 4 mm intervals. About 10 slices selected for each core sample. The diameter and length of the selected core samples were about 3.8 cm and 5.0 cm, respectively.

All CT data were obtained on conventional medical scanner. A high speed QX/i CT scanner was used to carry out the experiments. Scanner parameters were 120 kV x-ray tube voltage and the current used is 50 mA. Measurements were at room temperature on 0.6 mm slice thickness and 10 cm scan diameter. Image array size is 512 x 512, in which each pixel representing a volume element 0.2mm x 0.2mm x 0.6mm.

Discussion and result

The average CT no. were taken on the CT numbers obtained from the slices for each sample. Then the helium porosity, air permeability and grain density of each sample were used along with its averaged CT number to generate the correlation that shown in figures 1 and 2. The samples which contain limestone and dolestone were grouped as pure samples; whereas carbonate samples are consist of limestone, dolestone and anhydritic dolestone (figures 3 to 5). The correlation of porosity with its averaged CT no. for different rock types are shown in figure 2. Correlations in table 1 are generated to calculate porosity from CT number. However, for using results in table 3 and equation 6 in the generation of correlations, these parameters should be revised to evaluate and understand the effect of the photon energy of the scanning beam on CT no.. Thus a known sample was put on different tube voltage 80, 100 and 120 KV (figure 6).

Table 1: porosity calculation equations from CT no. for different lithologies

Correlation	Lithology
$\phi = -0.0337(CTno.) + 88.365$, $R^2 = 0.9554$	limestone
$\phi = -0.0372(CTno.) + 67.91$, $R^2 = 0.9186$	Dolestone
$\phi = -0.0234(CTno.) + 63.617$, $R^2 = 0.9013$	carbonate

As shown in figure 2, there are different trends of porosity versus CT no. for the limestone and dolestone samples. That is, regardless of high grain density, the CT no. of dolomite is less than limestone for the same porosity. It can be concluded that the grain density is not the only deterministic factor. So, there must be another parameter controlling CT number.

Table 2: porosity calculation equations for different lithologies

Correlation	Lithology
$\phi = (2622.11\text{-}CT_t)/2967.36$	limestone
$\phi = (2496.69\text{-}CT_t)/3676.47$	Dolestone
$\phi = (2718.68\text{-}CT_t)/4273.50$	carbonate

Table 3: CT air and Ct matrix calculated for different lithologies

CT_{matrix}	CT_{air}	Lithology
2622.11	-345.252	limestone
2496.69	-1179.78	Dolestone
2718.68	-1554.83	carbonate
-	-1000	standard
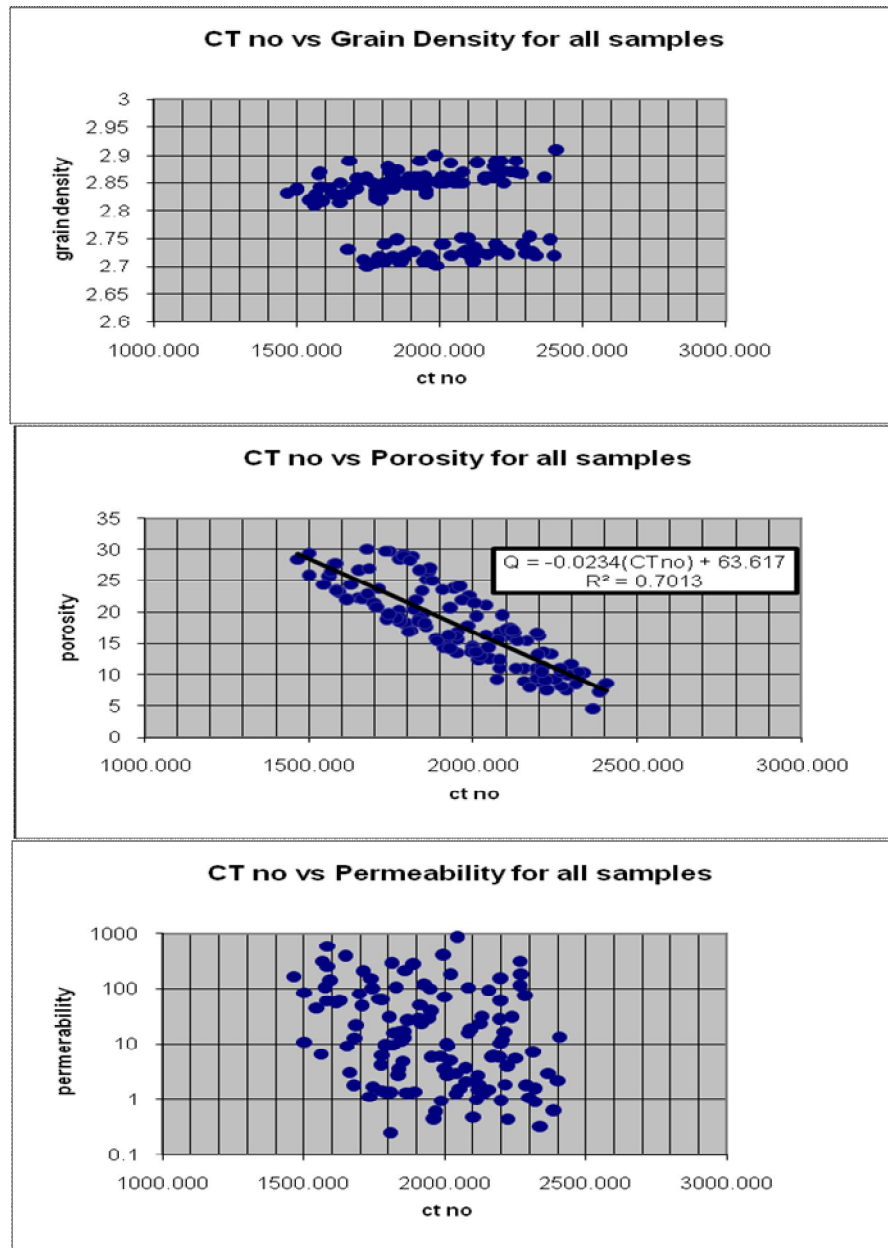
Figure 1: crossplot of CT no. and Petrophysical parameters
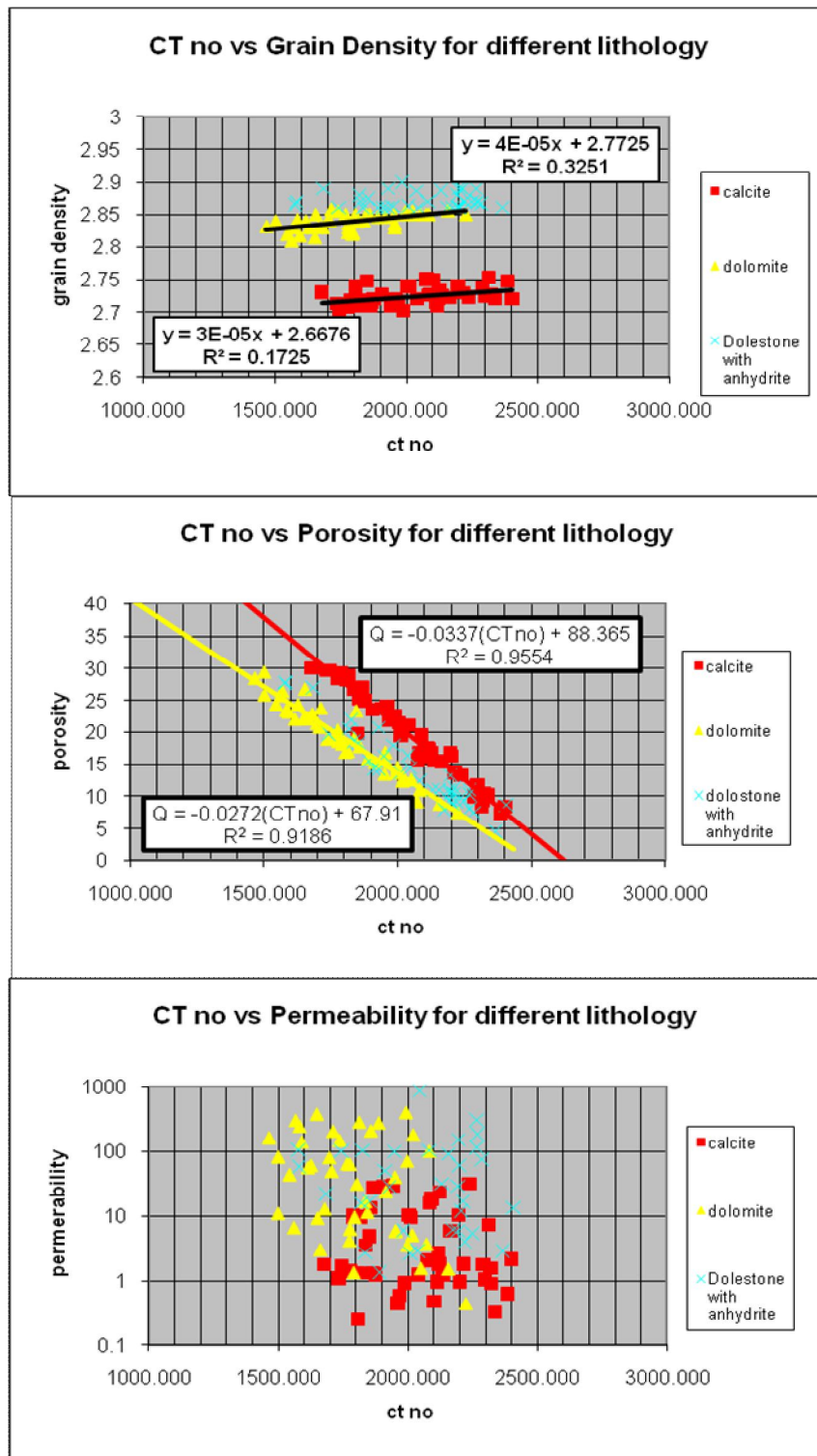
Figure 2: crossplot of CT no. and Petrophysical parameters for Limestone, Dolestone and dolestone with anhydrite

Seemingly this factor is the effective atomic number. Considering the related effective atomic numbers, it is obvious that the atomic number of dolomite is less than limestone (15.71 and 13.74 for calcite and dolomite, respectively). As in equation 4, the effect of effective atomic number is more than grain density, so that the CT no. for dolomite is less than that of limestone for the same porosity. The CT no. for the dolestone

and limestone groups is different in a given porosity. It is due to pore type differences between dolostone and limestone. So their differences increase by porosity enhancement in ø-CT plot. Considering figures 3 and 4, it shows that depending on the rock mineralogy there are two different pores types (commonly intercrystalline in dolostone and vuggy in limestone).
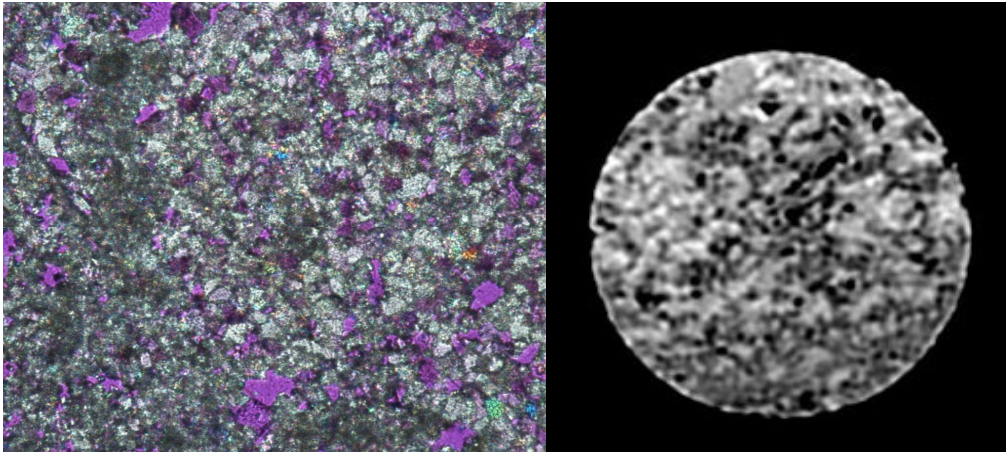
Figure 3: thin-section and CT images for Dolestone with high porosity
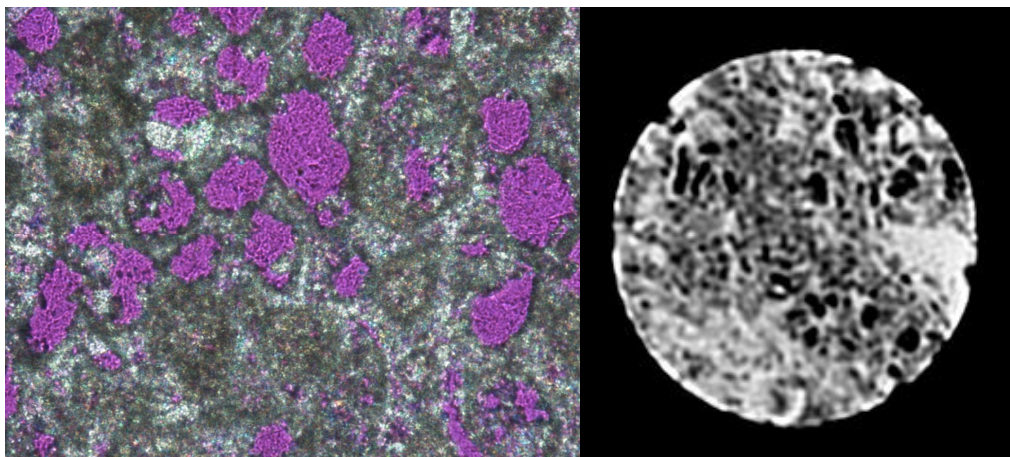
Figure 4: thin-section and CT images for Limestone with high porosity
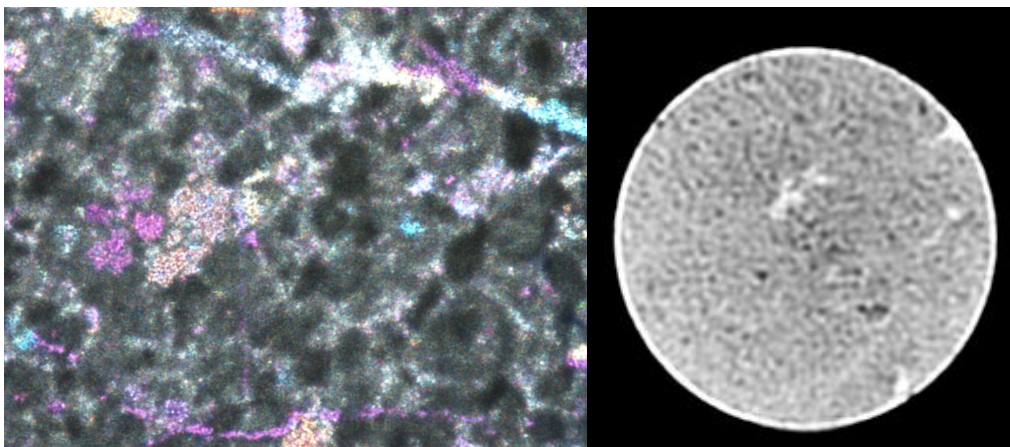
Figure 5: thin-section and CT image for fine grain Dolestone with coarse grain Anhydrite and Low porosity (Porosity 7.53%)
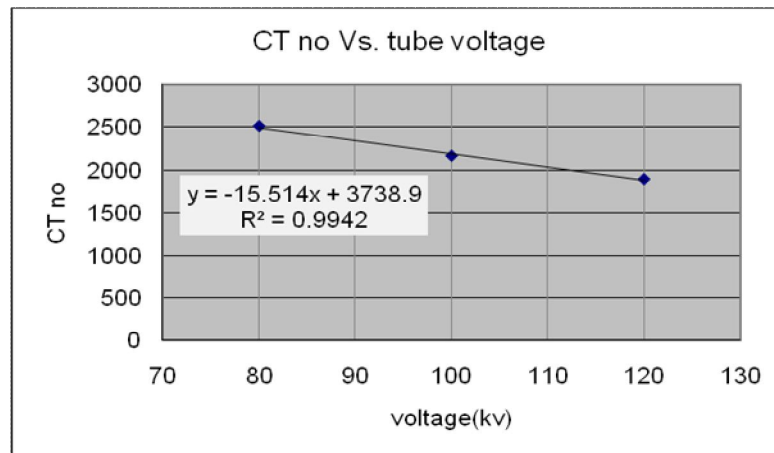
Figure 6: the linear changed CT no. with equipment tube voltage

Therefore, the lack of coincidence between object boundaries and pixel boundaries in limestone and dolestone groups could be related to the pore types. Explicitly, if the pore spaces are connected and continuous, there will have less noises and more coincidence of boundaries. Therefore, dolestone and limestone differences in ø-CT plot rises as the porosity increases. Consequently, pore type could be another parameter that affecting the CT no. trend in the ø-CT cross plot . This conclusion is obvious by considering and comparing figures 2b and figures 3 and 4 together.

The CT air in limestone is shown to be lower than the standard, whereas it is near the standard for dolestone due to good connection of pores (table 3). However, in higher and lower porosities (more than 27%, and less than10%) the noises and non-coincidence of object boundaries with pixel boundaries is going to be less effective for limestone and dolestone groups in ø-CT plot and they approach together as shown in figure 2b. Whereas, the CT matrix (0% porosity) in the same figure for limestone is more than that of dolestone which is due to high effective atomic number of calcite. Moreover, CT matrix and CT air are also obtained for carbonate group that differ from previous groups and it was due to the existence of anhydrite.

In the absence of the effect of atomic number, CT no. increases with grain density in each lithology (figure 2a). Our results also showed that CT no. has no correlation with permeability (figure 2c). Higher slope and coefficient of correlation in ø-CT no. cross plot than the ñ-CT no. cross plot for each lithology is indicative of higher porosity effects on the CT no. than the grain density (figure 2a and 2b).

In addition, a reverse linear relation exists between CT no. and CT-scan equipment tube voltage. This was obtained from the sample put under the different tube voltages as illustrated in figure 6. Effect of equipment tube voltage on CT no. was showed by this result.

Conclusion

There is high correlation coefficient in the developed correlations that indicates a good prediction of porosity for different lithology.

The results showed that the effect of atomic number on CT no. is more than the grain density.

CT no. is more affected by porosity than density of minerals.

Grain density and permeability have no good relation with CT no..

Pore type is another parameter affecting the CT no. with respect to porosity.

CT no. varies in indirect linear relation as photon energy changes.

References

Akin, S., Demiral, B., Okandan, E., 1996. A novel method of porosity measurement utilizing computerized tomography. In Situ 20, 347– 365.

Akin, S., Kovscek, A.R., 2003. Computed tomography in petroleum engineering research. In: Mees, F., Swennen, R., Van Geet, M., Jacobs, P. (Eds.), Application of X-ray Computed Tomography in the Geosciences. Special Publication - Geological Society of London, vol. 215, pp. 23– 38.

Akin, S., Schembre, J.M., Bhat, S.K., Kovscek, A.R., 2000. Spontaneous imbibition characteristics of diatomite. J. Pet. Sci. Eng. 25 (3 and 4), 149– 165.

Anderson, S.H., Gantzer, C.J., Boone, J.M., 1988. Rapid non destructive bulk density and soil water content determination by computer tomography. Soil Sci. Soc. Am. J. 52, 35– 40.

Ashbridge, D.A., Thorne, M.S., Rivers, M.L., Muccino, J.C., O'Day, P.A., 2003. Image optimization and analysis of synchrotron X-ray computed microtomography (CAT) data. Comput. Geosci. 29, 823– 836.

Coenen, J.G.C., Maas, J.G., 1994. Material classification by dual-energy computerized X-ray tomography. In: Proceedings on the International Symposium on Computerized Tomography for Industrial Applications, Berlin, pp. 120–127.

Murat D., 2001. Effect of pore size distribution on porosity measurement by computerized tomography, SCA 2001-49.

Hunt, P.K., Engler, P., and Bajsarowicz, C., 1988. Computed Tomography as a Core Analysis Tool: Applications, Instrument Evaluation, and Image Improvement Techniques: Journal of Petroleum Technology, vol. 40, no. 9, p. 1203-1210.

Johns, R. A., Steude, J.D., Castanier, L.M., Roberts, P.V., 1993. Non destructive measurements of fracture aperture in crystalline rock cores using X-ray computed tomography. J. Geophys. Res. 98, 1889–1900.

Peters, E.J., Afzal, N., 1992. Characterization of heterogeneities in permeable media with computed tomography imaging. J. Pet. Sci. Eng. 7, 283–296.

Moss, R.M., Pepin, G. P., Davis, L. A., 1990. Direct measurement of the constituent porosities in a dual porosity matrix, SCA conference paper number 9003.

Radaell F. i, 2004. Uncertainty reduction in the evaluation of poorly consolidated, thin bedded core using X-ray computed tomography, Symposium of the Society of Core Analysts held in Abu Dhabi, UAE, 5-9 October, 2004.

Sheppard, A.P., Sok, R.M., Averdunk, H., 2004. Techniques for image enhancement and segmentation of tomographic images of porous materials. Physica A 339, 145–151.

Ueta, K., Tani, K., Kato, T., 2000. Computerized X-ray tomography analysis of three-dimensional fault geometries in asementinduced wrench faulting. Eng. Geol. 56 (1 and 2), 197– 210.

Wellington, S.L., Vinegar, H.J., 1987. X-ray computerized tomography. Journal of Petroleum Technology 39, 885–898.

Withjack, E.M., 1988. Computed tomography for rock property determination and fluid flow visualization: SPE Formation Evaluation, vol. 3, no. 4, p. 696-704City